Impacts of connected and autonomous vehicles on the performance of signalized networks: A network fundamental diagram approach

December 2021

A Research Report from the Pacific Southwest Region University Transportation Center

Wen-Long Jin, Institute of Transportation Studies - UC Irvine

Ximeng Fan, Institute of Transportation Studies - UC Irvine

Pacific Southwest Region UTC
University Transportation Center

ITS·IRVINE
Institute of Transportation Studies

TECHNICAL REPORT DOCUMENTATION PAGE

1. Report No. PSR-19-32, TO 028	**2. Government Accession No.** N/A	**3. Recipient's Catalog No.** N/A
4. Title and Subtitle Impacts of connected and autonomous vehicles on the performance of signalized networks: A network fundamental diagram approach		**5. Report Date** 4/6/2022 **6. Performing Organization Code** N/A
7. Author(s) Wen-Long Jin https://orcid.org/0000-0002-5413-8377 Ximeng Fan https://orcid.org/0000-0002-3093-9815		**8. Performing Organization Report No.** TBD
9. Performing Organization Name and Address Institute of Transportation Studies University of California, Irvine 4070 Anteater Instruction and Research Bldg (AIRB) Irvine, CA 92697-3600		**10. Work Unit No.** N/A **11. Contract or Grant No.** USDOT Grant 69A3551747109
12. Sponsoring Agency Name and Address U.S. Department of Transportation Office of the Assistant Secretary for Research and Technology 1200 New Jersey Avenue, SE, Washington, DC 20590		**13. Type of Report and Period Covered** Final report (2/1/2020 –12/31/2021) **14. Sponsoring Agency Code** USDOT OST-R
15. Supplementary Notes N/A		

16. Abstract

Many eco-driving strategies through speed control using constrained optimization algorithms have proven effective on signalized roads. However, heuristic speed limit control strategies and understanding of their overall performance across congestion levels remain an unexplored topic. In this work, we systematically study the performance of an eco-driving strategy based on Vehicle-to-Infrastructure (V2I) communication via the advisory speed limit (ASL), a speed limit designed for individual vehicles based on the idea of making vehicles enter signalized intersections at saturated headway intervals. The theoretical performance of our algorithm to vehicle trajectories is analyzed across different congestion levels. By simulating with the BA Newell's car-following model, the simplified Gipps model, and the Krauss model, calculated network fundamental diagrams (NFDs) and results of the Virginia Tech Microscopic Energy and Emission (VT-micro) model reveal an improvement in system mobility by nearly 10% and a reduction in fuel consumption by up to about 45% in the saturated condition. We further consider different market penetration rates (MPRs) and ASL implementation areas and show our algorithm can lead to about 35% fuel consumption reduction even with a 10% MPR. We recommend an ASL implementation area of about 100 meters, which can well balance the algorithm efficacy and computation cost.

17. Key Words Eco-driving, Advisory speed limit, Network fundamental diagram, Fuel consumption, Market penetration rate, ASL implementation area	**18. Distribution Statement** No restrictions.		
19. Security Classif. (of this report) Unclassified	**20. Security Classif. (of this page)** Unclassified	**21. No. of Pages** 44	**22. Price** N/A

Form DOT F 1700.7 (8-72) Reproduction of completed page authorized

Contents

List of figures

List of tables

About the Pacific Southwest Region University Transportation Center

The Pacific Southwest Region University Transportation Center (UTC) is the Region 9 University Transportation Center funded under the US Department of Transportation's University Transportation Centers Program. Established in 2016, the Pacific Southwest Region UTC (PSR) is led by the University of Southern California and includes seven partners: Long Beach State University; University of California, Davis; University of California, Irvine; University of California, Los Angeles; University of Hawaii; Northern Arizona University; Pima Community College.

The Pacific Southwest Region UTC conducts an integrated, multidisciplinary program of research, education and technology transfer aimed at *improving the mobility of people and goods throughout the region.* Our program is organized around four themes: 1) technology to address transportation problems and improve mobility; 2) improving mobility for vulnerable populations; 3) Improving resilience and protecting the environment; and 4) managing mobility in high growth areas.

U.S. Department of Transportation (USDOT) Disclaimer

The contents of this report reflect the views of the authors, who are responsible for the facts and the accuracy of the information presented herein. This document is disseminated in the interest of information exchange. The report is funded, partially or entirely, by a grant from the U.S. Department of Transportation's University Transportation Centers Program. However, the U.S. Government assumes no liability for the contents or use thereof.

California Department of Transportation (CALTRANS) Disclaimer

The contents of this report reflect the views of the authors, who are responsible for the facts and the accuracy of the information presented herein. This document is disseminated under the sponsorship of the United States Department of Transportation's University Transportation Centers program, in the interest of information exchange. The U.S. Government and the State of California assumes no liability for the contents or use thereof. Nor does the content necessarily reflect the official views or policies of the U.S. Government and the State of California. This report does not constitute a standard, specification, or regulation. This report does not constitute an endorsement by the California Department of Transportation (Caltrans) of any product described herein.

Disclosure

Principal Investigator, Wen-Long Jin, and Graduate Student Researchers, Ximeng Fan, conducted this research titled, "Impacts of connected and autonomous vehicles on the performance of signalized networks: A network fundamental diagram approach" at the Department of Civil and Environmental Engineering, College of Engineering, University of California, Irvine. The research took place from 2/1/2020 to 12/31/2021 and was funded by a grant from the California Department of Transportation in

the amount of $91,326. The research was conducted as part of the Pacific Southwest Region University Transportation Center research program.

Acknowledgements

This project was funded by a grant from the Pacific Southwest Region University Transportation Center (PSR), supported by Caltrans through the University Transportation Center research program. The authors would like to express their gratitude to the PSR and Caltrans for their support of university-based transportation research, particularly for supporting this project.

Abstract

Many eco-driving strategies through speed control using constrained optimization algorithms have proven effective on signalized roads. However, heuristic speed limit control strategies and understanding of their overall performance across congestion levels remain an unexplored topic. In this work, we systematically study the performance of an eco-driving strategy based on Vehicle-to-Infrastructure (V2I) communication via the advisory speed limit (ASL), a speed limit designed for individual vehicles based on the idea of making vehicles enter signalized intersections at saturated headway intervals. The theoretical performance of our algorithm to vehicle trajectories is analyzed across different congestion levels. By simulating with the BA Newell's car-following model, the simplified Gipps model, and the Krauss model, calculated network fundamental diagrams (NFDs) and results of the Virginia Tech Microscopic Energy and Emission (VT-micro) model reveal an improvement in system mobility by nearly 10% and a reduction in fuel consumption by up to about 45% in the saturated condition. We further consider different market penetration rates (MPRs) and ASL implementation areas and show our algorithm can lead to about 35% fuel consumption reduction even with a 10% MPR. We recommend an ASL implementation area of about 100 meters, which can well balance the algorithm efficacy and computation cost.

Keywords: Eco-driving, Advisory speed limit, Network fundamental diagram, Fuel consumption, Market penetration rate, ASL implementation area

Impacts of connected and autonomous vehicles on the performance of signalized networks: A network fundamental diagram approach

Executive Summary

In this project, we formulate and analyze an eco-driving strategy based on Vehicle-to-Infrastructure (V2I) communication via the advisory speed limit (ASL), a speed limit designed for individual vehicles based on the idea of making vehicles enter signalized intersections at saturated headway intervals. We analytically and numerically show how our algorithm can work at different congestion levels. We further study how market penetration rates (MPRs) (the proportion of connected vehicles that adopt the ASL) and the ASL implementation area (the area in which connected vehicles will adopt the ASL) can affect the efficacy of our algorithm.

Advisory speed limit (ASL) algorithm

The algorithm provides an ASL to each connected vehicle, which is calculated with the idea that vehicles at signalized intersections should enter the intersection at saturation headway intervals in the phase time.

Steps of the ASL algorithm

The algorithm begins to function in a connected vehicle when it enters the ASL implementation area, i.e., the area in which connected vehicles can receive the ASL, and the entire algorithm consists of three steps:

1. We calculate the desired arrival time based on the speed limit.
2. We calculate the desired arrival time based on the minimum headway to front vehicles.
3. We calculate the ASL with the desired arrival time and the distance to the intersection.

Implementations of the algorithm:

We consider two implementations of the proposed algorithm:

- The static ASL
- The dynamic ASL

Car-following models and evaluation indicator choice

We choose the BA Newell's car-following model, the simplified Gipps model, and the Krauss model to simulate vehicles' movements. All these models are safety-stopping distance

car-following models, in which collisions are avoided and meaningful fundamental diagrams are guaranteed. We choose network fundamental diagrams to indicate system mobility and fuel consumption to indicate environmental impacts.

Simulation and results

We choose Python to simulate vehicles' movements before and after applying our algorithm. We construct a signalized ring road with one lane and one typical three-color traffic light, on which vehicles are initially distributed evenly. After the simulation begins, the signal starts with a green interval, and vehicles move clockwise. We assume all drivers are aggressive and traverse the density from 0 to near jam density by changing the vehicle number. We test three conditions: 1. no control, 2. the static ASL, 3. the dynamic ASL. We then investigate how our algorithm works with 0.1, 0.3, 0.7, and 1 MPRs. We further change the ASL implementation area from $10m$ to $300m$ at intervals of $10m$ to see the performance of the dynamic ASL with different ASL implementation areas. Results show that:

- From the perspective of system mobility, the static ASL is unlikely to have a positive effect, it may diminish the system mobility. The dynamic ASL can improve the system mobility in the saturated condition by nearly 10%.
- From the perspective of fuel consumption, the dynamic ASL can reduce fuel consumption by up to 45% in the saturated condition.
- Both the improvement rate of system mobility and the reduction rate of fuel consumption is positively related to the MPR. The improvement rate of system mobility is not obvious when the MPR is low, however, fuel consumption can reduce by about 35% with only 0.1 MPR.
- We recommend the ASL implementation area to be approximate $100m$, which can guarantee control results as well as reduce computation costs.

1. Introduction

In 2018, the transportation sector is the largest source of greenhouse gas emissions accounting for 28% of all the emissions (Agency, 2018). Americans wasted nearly 4.8 billion hours and 1.9 billion gallons of fuel sitting in traffic (Milikowsky, 2013). With the urgent need to reduce transportation fuel consumption, the concept of 'eco-driving' was proposed. It is an initiative that has seen widespread attention in the past decade (Alam, 2014).

According to (Sivak & Schoettle, 2012), eco-driving is composed of a series of decisions that can affect the fuel economy. The decisions can be categorized into three groups, namely strategic decisions, tactical decisions, and operational decisions. Strategic decisions are about vehicle selection and maintenance as well as fuel selection (Anandarajah, et al., 2013) (Huang, et al., 2015) (Zhen & Wang, 2015). Admittedly, choosing low-displacement vehicles can reduce fuel consumption, but at the cost of lower horsepower and worse acceleration performance (Cheah, et al., 2009). Investment and studies on the new vehicle and fuel technologies have a broad and significant impact, but it takes a relatively long time for their effects to take place (Anandarajah, et al., 2013). Tactical decisions relate to route planning and weight, such as the trade-off between arterial routes and highways, sacrificing time or distance in exchange for saving fuel (Ahn & Rakha, 151-167). Operational decisions relate to driving styles. Compared with the above two, operational decisions have more immediate impacts and are possible to reduce fuel consumption without increasing travel time or distance. Therefore, we narrow eco-driving to driving behaviors in this study.

From the perspective of driving behaviors, eco-driving can be regarded as an approach that involves (1) accelerating moderately, anticipating traffic flow and signals, thereby avoiding sudden starts and stops; (2) maintaining an even driving pace, driving at or safely below the speed limit; and (3) eliminating excessive idling (Barkenbus, 2010). Vehicles on urban roads are regularly interrupted by traffic signals, causing large variations in speed and idling time, and additional fuel consumption. Therefore, eco-driving strategies have a large impact when being applied at signalized intersections. Those strategies are further supported by the advancement of communication technologies and connected vehicles (CVs), vehicles capable of accessing the Internet and collecting real-time data (Coppola & Morisio, 49). These technologies enable Vehicle-to-Infrastructure (V2I) and Vehicle-to-Vehicle (V2V) communication, providing a platform for applying eco-driving strategies at signalized intersections via the availability of Signal Phase and Timing (SPaT) information and inter-vehicle information within some distance, for example, dedicated short-range communication (DSRC) transmission range (Kenney, 2011).

Various eco-driving strategies have proposed speed-control algorithms in signalized networks that adapt to signal timing and smooth vehicle trajectories. (Mandava, et al., 2009) developed an arterial speed planning algorithm aiming at minimizing the

acceleration/deceleration rate for human drivers traveling in signalized networks. (Rakha & Kamalanathsharma, 2011) developed a strategy to work out the most fuel-optimal speed profile for a vehicle to go through the intersection utilizing V2I communication capabilities. Taking advantage of V2I communication technology, the Green Light Optimal Speed Advisory (GLOSA) system was also developed. It offers each driver a speed or an acceptable speed range when approaching a signalized intersection to make better use of green intervals (Katsaros, et al., 2011) (Seredynski, et al., 2013) (Eckhoff, et al., 2013).

Accurate speed control, however, requires a high market penetration rate and is very sensitive to errors in the external environment and communication devices. Instead, speed limit control only works out speed limits according to signal status and traffic conditions, while still allowing vehicles to follow their preceding vehicles according to local information. From this perspective, speed limit control is more robust subject to changes in the external environment. Speed limit control can be divided into variable speed limit (VSL) control (Chen, et al., 2020) and advisory speed limit (ASL) control (Yang & Jin, 2014) (Ubiergo & Jin, 2016). VSL is a location-dependent speed limit, and all the vehicles in one segment follow one speed limit regardless of their own situation. On the other hand, ASL is geared towards individual control, providing each vehicle with its own speed limit. (Yang & Jin, 2014) initially proposed an ASL algorithm attempting to smooth vehicle trajectories, maintain the average speed, allow minimal speed limit variations, and function under different market penetration rates; and detected its short-time impact on fuel consumption and emission. (Ubiergo & Jin, 2016) proposed an idea of making connected vehicles enter the intersection during the green at saturation headway intervals through ASL and examined the short-time performance of such ASL in some under-critical conditions. So far, there still lacks research on the ASL algorithm's long-time control effect under different congested levels.

The impact of eco-driving strategies can be evaluated by system mobility and environmental impacts. System mobility can be characterized by network fundamental diagrams. (Godfrey, 1969) first indicated that there exists a reproducible and well-defined relation between average flow and average density in an urban network. Such a relation is called the macroscopic fundamental diagram (MFD), and it has shown substantial potential in informing traffic control (Keyvan-Ekbatani, et al., 2012) (Zheng, et al., 2012) (Khondaker & Kattan, 2015). (Jin, et al., 2013) further defined stationary states, where the MFDs should be calculated, in signalized networks as asymptotic periodic traffic patterns, and (Jin & Yu, 2015) proved that such periods should be the cycle length or integer multiples of the cycle length. Environmental impacts are often evaluated through models such as the Comprehensive modal emissions model (CMEM) (Barth, et al., 2000), mobile source emission factor model (MOBILE) (others, 2000), and Virginia Tech microscopic energy and emission model (VT-micro model)

(Ahn, et al., 2002). These models collaboratively provide researchers a measure of the amount of fuel or emission saved through their control algorithms.

In this paper, we formulate and analyze an eco-driving strategy based on Vehicle-to-Infrastructure (V2I) communication via the ASL with the idea that all vehicles should enter the intersection at saturation headway intervals in the phase time (Ubiergo & Jin, 2016), i.e., the minimum constant headway that can be achieved by a saturated, stable moving queue of vehicles passing through the signal (McShane & Roess, 1990). The algorithm begins to function when a connected vehicle enters the ASL implementation area, i.e., the area in which connected vehicles can receive the ASL. The algorithm consists of three steps: 1. we calculate the desired arrival time based on the speed limit; 2. we calculate the desired arrival time based on the minimum headway to front vehicles; 3. we calculate the ASL with the desired arrival time and the distance to the intersection. We analytically illustrate the performance of two implementations, i.e., static ASL and dynamic ASL, of our algorithm at different congestion levels from the perspective of vehicle trajectories. The static ASL is calculated only when a connected vehicle enters the ASL implementation area, while the dynamic ASL keeps updating once it enters the ASL implementation area. We then adopt the BA Newell's car-following model (Jin & Laval, 2018), simplified Gipps model (Gipps, 1981) (Treiber & Kesting, 2013), and Krauss model (Krauss, et al., 1997) (Krauss, 1998) to describe vehicles' movements, and the VT-micro model (Ahn, et al., 2002) to calculate the fuel consumption. We evaluate the long-time performance of our ASL algorithm from the perspectives of system mobility and environmental impacts. Finally, we examine how different market penetration rates (MPRs) and the length of ASL implementation areas can impact the efficacy of our algorithm.

Our work is an extension of (Ubiergo & Jin, 2016), in which the idea of making vehicles enter the intersection at saturated headway intervals was proposed. Our study provides detailed steps and formulas for the algorithm and discusses different implementations of the algorithm. On the one hand, for a connected vehicle, our algorithm alleviates the requirement for knowledge of the desired arrival time of its preceding vehicles and reduces the information necessary for the calculation of its ASL to its location, signal status, and the number of vehicles in front, all of which are simple and easily measurable. On the other hand, we propose the use of NFDs to study long-time impacts on system mobility of dynamic ASL at different congestion levels.

The rest of this paper is organized into 6 sections. In Section 2, we will set up the study, propose the principles and assumptions as well as analyze the existed ASL algorithm. In Section 3, we will extend the ASL algorithm and analytically illustrate the effects of extended ASL. In Section 4, we will introduce driving behaviors at signalized roads as well as performance measurements of our algorithm. In Section 5, we will set up the simulation, conduct it and analyze the corresponding results. In Section 6, we will take MPRs as well as ASL

implementation areas into consideration and detect their impacts on the efficiency of our algorithm. Finally, we will summarize the conclusions and discuss some potential extensions of our research.

2. Setup and background of advisory speed limit (ASL) study

In this chapter, we illustrate the setup of the system where we design the ASL and introduce its rules and assumptions.

2.1 Illustration of a signalized road with the ASL implementation area

We utilize Figure 1 to illustrate a one-lane road with one fixed time three-color signal and the ASL implementation area, i.e., the area in which connected vehicles will adopt the ASL. Vehicles on the road include connected vehicles (shown in red) and non-connected ones (shown in white). All vehicles are labeled in order from the downstream to the upstream. Once a connected vehicle enters the ASL implementation area, the ASL algorithm begins to function.

Figure 1: Illustration of a signalized road with the ASL implementation area

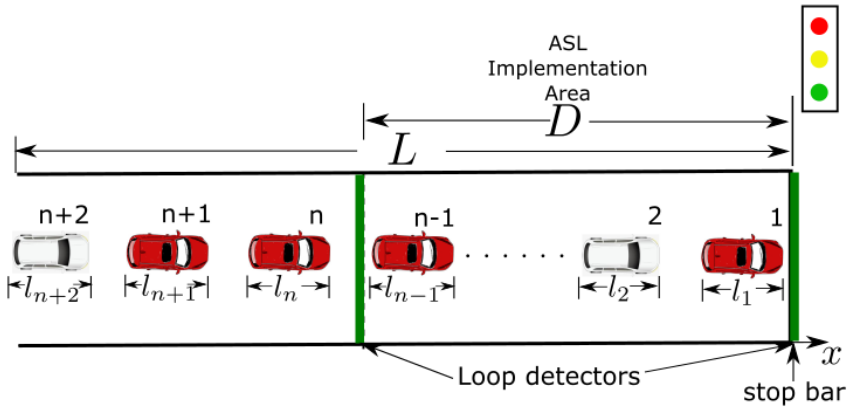

Apart from the notations marked in Figure 1, more detailed notations we are going to utilize are listed in Table 1.

Table 1. A list of notations

Variables	Definitions	Variables	Definitions
Length and position variables			
L	Road length	l_n	Length of vehicle n
s_0	Minimum clearance	ζ	Jam spacing
D	ASL implementation area length	γ	Transmission range
$x_n(t)$	Position of vehicle n at time t		

Time variables			
t	Time	Δt	Time step
τ	Time gap	t_{re}	Reaction time
B	Cycle length	G	Green interval
Y	Yellow plus all-red interval	R	Red interval
σ	Simulation duration	h	Saturation headway
h'_n	Headway between vehicle n and $n+1$		
t_n^*	The time when vehicle n enters the ASL implementation area		
$\Phi_n(t)$	Desired arrival time of vehicle n at time t		
$T_n(N)$	Period of vehicle n's speed in stationary states when N vehicles are in the system		
$T_{sys}(N)$	Period of the system average speed when N vehicles are in the system		
Speed and acceleration variables			
v_f	Original speed limit	w	Shock wave in congested traffic
a_0	Bounded acceleration	b	Bounded deceleration
$v_n(t)$	Speed of vehicle n at time t	$a_n(t)$	Acceleration of vehicle n at time t
$U_n(t)$	ASL of vehicle n at time t		
Variables	**Definitions**	**Variables**	**Definitions**
$\bar{v}_{ind.n}(m)$	The average speed of vehicle n in the mth cycle		
$\bar{v}_{sys}(m)$	System average speed in the mth cycle		
Other variables			
π	$=(G+Y)/B$, phase ratio	V_n	Fuel consumption of vehicle n
q_c	Capacity		
$\bar{V}_n$	The average fuel consumption of vehicle n to move a unit distance in one period		
J_t^n	Number of vehicles in front of vehicle n at time t		

Intuitively, we should make connected vehicles adopt ASL algorithms as early as possible based on satisfying the constraints of the road length and communication technology so that drivers have more time to adjust speeds. In this study, a DSRC network is adopted (Kenney, 2011). Thus, an optimization problem can be formulated as:

$$\max D \quad s.t. \begin{cases} D \le \gamma \\ D \le L \\ D \ge 0 \end{cases}, \tag{1.}$$

which means that the ASL implementation area should be the smaller value between road length L and transmission range γ.

2.2 Rules and assumptions

We consider our algorithm should follow the following rules:

- The algorithm should improve the braking and acceleration process before signalized intersections, leading to smoother trajectories with less variation of velocity.

- The algorithm is designed based on the ideal condition presented in (Ubiergo & Jin, 2016) that all connected vehicles enter the intersection in phase at saturation headway intervals.

- The efficiency of the algorithm should increase with a higher market penetration rate (MPR). Even if only one connected vehicle in the system adopts our algorithm, our algorithm should have certain effects.

- The required information should be as simple and measurable as possible.

In addition, we have the following assumptions for our study:

- We assume that vehicles move on a one-lane road, and strictly follow the first in first out (FIFO) rule.

- We assume that the parameters, including length, maximum acceleration and maximum deceleration, are the same for all vehicles. And initially, vehicles are evenly distributed on the road.

3. Advisory speed limit (ASL) algorithm

In this chapter, we present the algorithm and analytically illustrate the impacts of our algorithm on vehicle trajectories at different congestion levels.

3.1 Algorithm design

Based on the core idea of helping vehicles avoid entering the intersection at red intervals and reduce idling time, we formulate an ASL algorithm at discrete time steps. Note that this algorithm is only applied to connected vehicles in the ASL implementation area. Whether a vehicle is a non-connected vehicle, or it is not in the ASL implementation area, it will follow the original speed limit v_f .

For each connected vehicle in the ASL implementation area, we can detect the number of vehicles in front of it. We assume vehicle n is a connected vehicle entering the ASL implementation area, and the signal begins with the green interval at $t = 0$. Current time is denoted as t, the number of vehicles in front of vehicle n at time t is denoted as J_t^n. As shown in Figure 2, the whole process can be summarized into three steps at each discrete time step.

Figure 2: Flow chart of the ASL algorithm

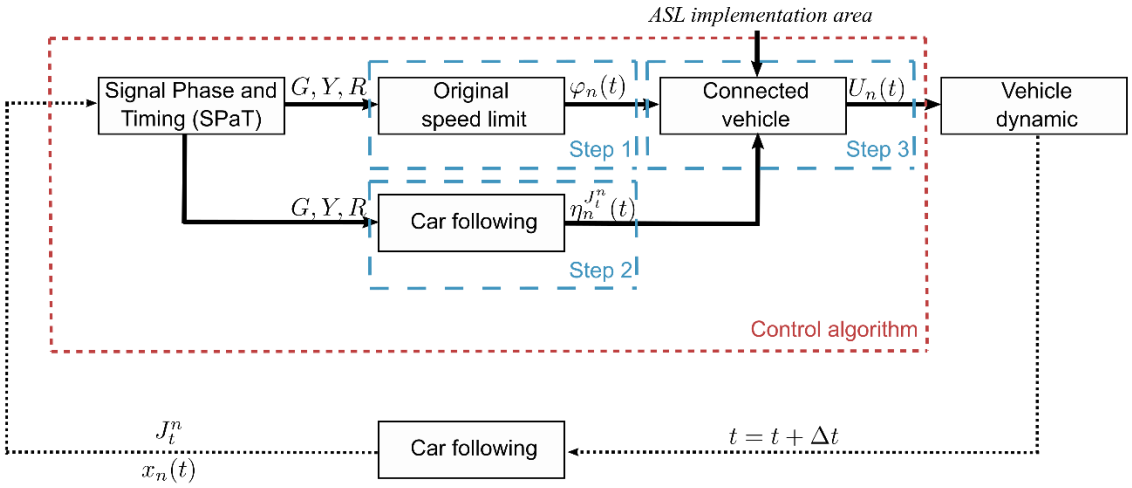

1. Vehicle speeds cannot exceed the original speed limit. The earliest time vehicle n can enter the intersection can be calculated based on the original speed limit and the signal as follows:

$$\varphi_n(t) = \begin{cases} H_n(t), & \frac{H_n(t)}{B} - \left\lfloor \frac{H_n(t)}{B} \right\rfloor \leq F_n(t) \\ \left(\left\lfloor \frac{H_n(t)}{B} \right\rfloor + 1 \right) B, & \text{otherwise} \end{cases} \quad (2.)$$

$$H_n(t) = t + \frac{L - x_n(t)}{v_f}, \quad (3.)$$

where L is road length, v_f is the original speed limit and $x_n(t)$ is the position of vehicle n at time t. $F_n(t)B$ is the time during which there will be no vehicle stops at the stop line. Note that unlike the effective green time, i.e., the amount of time that vehicles can departure at a rate of one vehicle every h seconds (McShane & Roess, 1990), $F_n(t)B$ only focuses on whether vehicles can cross the stop line, regardless of the rate. Aggressive drivers will choose to cross the intersection at their first chance once they enter the intersection at phase, thus $F_n(t)B = \pi B$. Non-aggressive drivers will choose to stop at their first chance (Morales Fresquet & Jin, 2018). At the time point when the signal changes to yellow from green, they will choose to stop once the distance to the intersection is enough for them to brake. We assume the reaction time is t_{re}, and the braking distance and the time they need for braking can be written as $t_{re}v_n(t) + \frac{v_n(t)^2}{2b_0}$ and $t_{re} + \frac{v_n(t)}{b_0}$ respectively. Thus, a non-aggressive driver is impossible to cross the

stop line in one cycle after $G + t_{re} + \frac{v_n(t)}{b_0}$ and $F_n(t)B = G + t_{re} + \frac{v_n(t)}{b_0}$ for non-aggressive drivers, as follows:

$$F_n(t) = \begin{cases} \pi, & \text{For aggressive drivers} \\ \dfrac{G + t_{re} + \dfrac{v_n(t)}{b_0}}{B}, & \text{For non} - \text{aggressive drivers} \end{cases} \quad (4.)$$

2. The vehicle should obey the car-following rule, as Figure 3 shows. The ideal condition is that connected vehicles in the ASL implementation can enter the intersection at saturation headway (h) intervals. Meanwhile, if a vehicle is expected to enter the intersection at the end of one phase, the vehicle behind it can enter the intersection at the starting point of the next green interval. From this perspective, the earliest time vehicle n can enter the intersection can be calculated as follows:

Figure 3: Illustration of the desired arrival time of vehicle n based on front vehicles

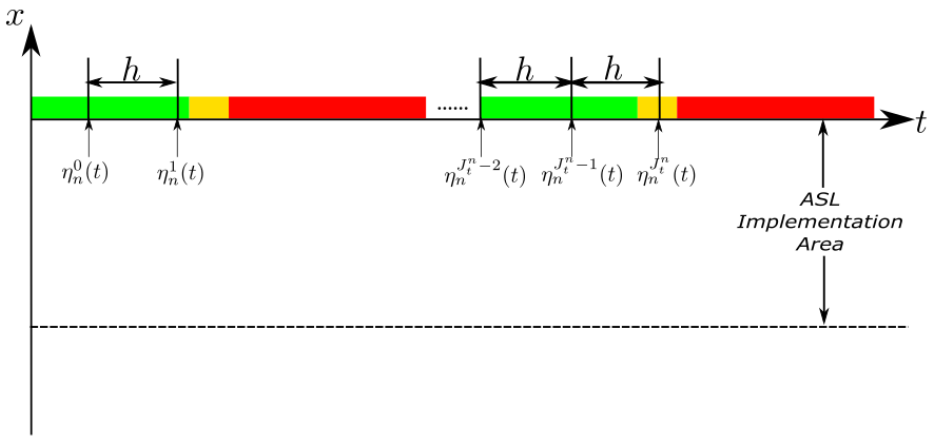

$$\eta_n^j(t)_{j\in[1,J_t^n]} = \begin{cases} \eta_n^{j-1}(t) + h, & \dfrac{\eta_n^{j-1}(t)+h}{B} - \left\lfloor \dfrac{\eta_n^{j-1}(t)+h}{B} \right\rfloor \le F_n(t) \\ \left(\left\lfloor \dfrac{\eta_n^{j-1}(t)+h}{B} \right\rfloor + 1 \right) B, & \text{otherwise} \end{cases} \quad (5.)$$

where h is the saturation headway, j increases from 1 to J_t^n, and $\eta_n^{J_t^n}(t)$ is the final result we want to obtain. Note that if there are no vehicles in front of vehicle n ($J_t^n = 0$), then $\eta_n^0(t) = t$ if the current signal is in phase, otherwise it is equal to $\left(\left\lfloor \frac{t}{B} \right\rfloor + 1 \right) B$.

3. Finally, we calculate the advisory speed at the next time step. The time left for vehicle n to reach the intersection is $(\max\{\eta_n^{J_t^n}(t), \varphi_n(t)\} - t)$ and the distance it needs to cover is $(L - x_n(t))$. Therefore, the ASL of vehicle n can be calculated as follows:

$$U_n(t) = \frac{L - x_n(t)}{\max\left\{\eta_n^{J_t^n}(t), \varphi_n(t)\right\} - t}, \quad (6.)$$

The original speed limit will then be replaced by the ASL. There are two ways of implementing our ASL algorithm: 1. calculate it only when the vehicle enters the ASL implementation area (refers to as 'statistic ASL'); 2. keep updating it once the vehicle enters the ASL implementation area, as shown by the dashed lines in Figure 2 (refers to as 'dynamic ASL'). More discussion about this will be presented in the following.

In summary, once a connected vehicle enters the ASL implementation area, we can know the number of vehicles in front of it with the loop detectors at the entrance of the ASL implementation area and before the stop line. At the moment the connected vehicle enters the ASL implementation area, our algorithm will calculate its desired arrival time based on the original speed limit and the number of vehicles in front of it. This desired arrival time indicates the earliest time point at which the connected vehicle can go through the intersection without stopping. The ASL is then calculated by dividing the remaining distance to the intersection by the remaining time until the desired arrival time. If we consider the statistic ASL, this value will not be updated and the connected vehicle's speed will not exceed this value in the remaining distance to the intersection. If we consider the dynamic ASL, the ASL will be calculated and updated at each time step, and the value of the ASL may change from time to time; the connected vehicle will always follow the newest ASL in the remaining distance to the intersection.

Our algorithm only requires three easily measurable inputs: position, signal status, and the number of vehicles in front to calculate the ASL of a vehicle. Calculating desired arrival time through the iteration method makes full use of the phase. Meanwhile, both aggressive drivers and non-aggressive drivers are considered in the algorithm.

3.2 Analytical trajectories after applying the ASL

We consider two different implementations of the ASL: the static ASL and the dynamic ASL. The static ASL is calculated only when a connected vehicle enters the ASL implementation area, and the dynamic ASL is continuously updated when the vehicle is in the implementation area. Here we assume that our algorithm can fully function, and vehicles are all connected, and illustrate how it works with three vehicles, denote as vehicles n to $n + 2$, which are entering

the ASL implementation area at the original speed limit v_f. The analysis is shown in Figure 4 to Figure 6.

First, we discuss the under-saturated condition, as Figure 4a, Figure 4c, and Figure 4d show, we plot vehicle trajectories for the following conditions: no ASL is applied; static ASL is applied; dynamic ASL is applied. From Figure 4a it can be found that lost time exists in start-up behaviors after long-time stopping due to the reaction and accelerating process, and the actual headway between vehicle n and vehicle $n+1$, marked as h'_n, is greater than the saturation headway.

When the static ASL is applied, as shown in Figure 4c, all three vehicles can move at their own ASLs $U_n(t_n^*)$, $U_{n+1}(t_{n+1}^*)$, and $U_{n+2}(t_{n+2}^*)$, as they just enter the ASL implementation area, and all these three values are smaller than v_f. However, vehicle $n+1$ will encounter a shock wave caused by the deceleration of vehicle n shortly after it enters the ASL implementation area and decelerates to $U_n(t_n^*)$. Vehicle n will accelerate from $U_n(t_n^*)$ when it crosses the intersection. However, after vehicle n crosses the intersection, vehicle $n+1$ is unable to re-accelerate to v_f before entering the intersection because its speed is constrained by $U_{n+1}(t_{n+1}^*)$ (green line), and it will enter the intersection at $U_{n+1}(t_{n+1}^*)$. The same condition also occurs to vehicle $n+2$ (orange line), and it can only enter the intersection at $U_{n+2}(t_{n+2}^*)$. As a result, the actual headway between two adjacent vehicles, h'_n and h'_{n+1}, will always be greater than the saturation headway. Therefore, also stopping behaviors are eliminated and trajectories are smoother, the lost time not only will not decrease but may increase.

With the application of the dynamic ASL, as shown in Figure 4d, the trajectory of vehicle n, as well as the trajectories of vehicle $n+1$ and $n+2$ before vehicle n crosses the intersection, are the same as those when the static ASL is applied. However, the dynamic ASL for the following vehicles will update after their front vehicles cross the intersection. Thus vehicle $n+1$ (green line) and vehicle $n+2$ (orange line) can re-accelerate to the original speed limit before entering the intersection. Although the headway between vehicle n and vehicle $n+1$ is still greater than the saturation headway, the headway between vehicle $n+1$ and $n+2$ can reach the saturation headway. Therefore, the accelerating process of vehicles $n+1$ and $n+2$ will be reduced, the trajectories will be smoother, and the lost time at the intersection will be reduced.

Figure 4: Trajectories analysis of the ASL algorithm in the under-saturated condition

a) Trajectories of vehicles without control

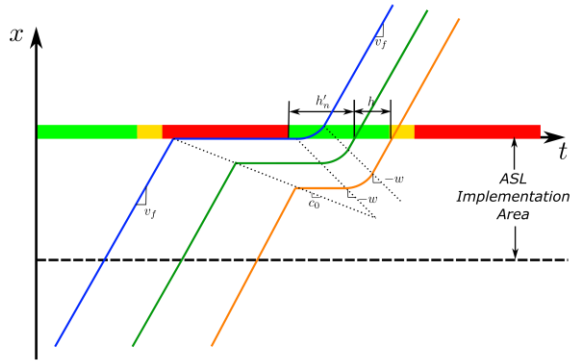

b) Fundamental diagram for calculating ASL

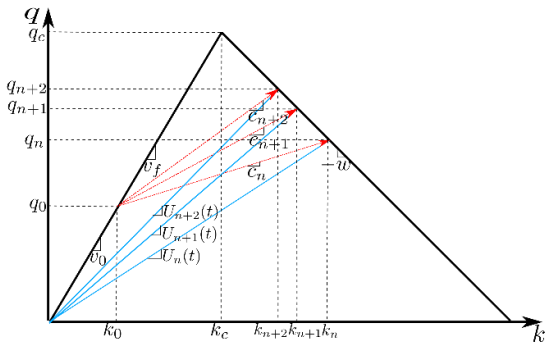

c) Trajectories after applying ASL statically

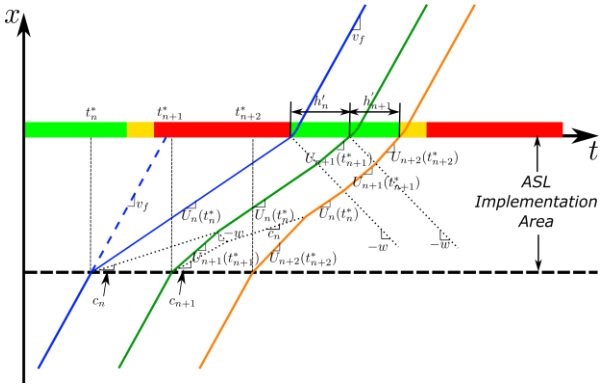

d) Trajectories after applying ASL dynamically

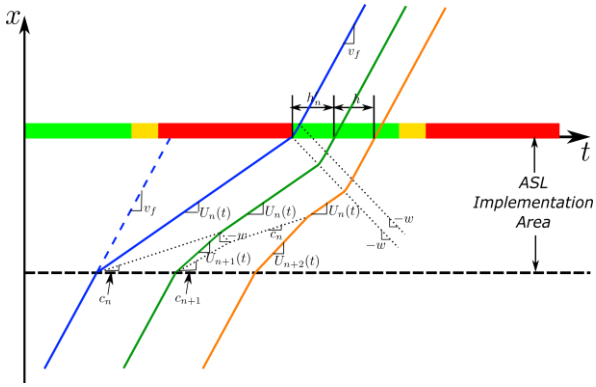

We then take the critical density as an example to study how our algorithm works in the saturated condition, as Figure 5c and Figure 5d show. The headway between two adjacent vehicles is the saturation headway before vehicle n enters the ASL implementation area. Vehicle $n+1$ (green lines) and vehicle $n+2$ (orange lines) will encounter the shock wave and decelerate before they enter the ASL implementation area. When the static ASL is applied, as shown in Figure 5c, Vehicle $n+1$ and $n+2$ still can only enter the intersection at $U_{n+1}(t_{n+1}^*)$ and $U_{n+2}(t_{n+2}^*)$, respectively, and the headway between two adjacent vehicles will be greater than the saturation headway. The trajectories in the saturated condition, as shown in Figure 5d, are the same as those in the under-saturated condition after vehicle n crosses the intersection.

Figure 5: Trajectories analysis of the ASL algorithm in the saturated condition

a) Trajectories of vehicles without control b) Fundamental diagram for calculating ASL

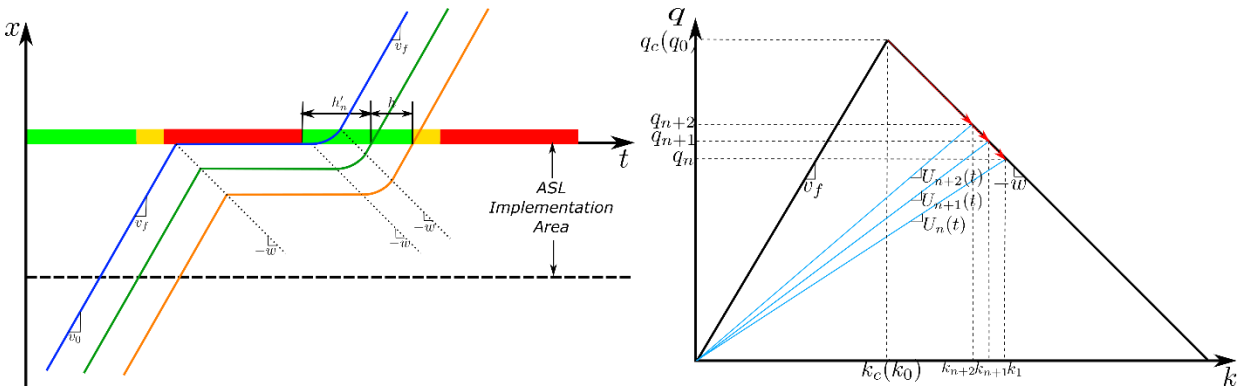

c) Trajectories after applying ASL statically d) Trajectories after applying ASL dynamically

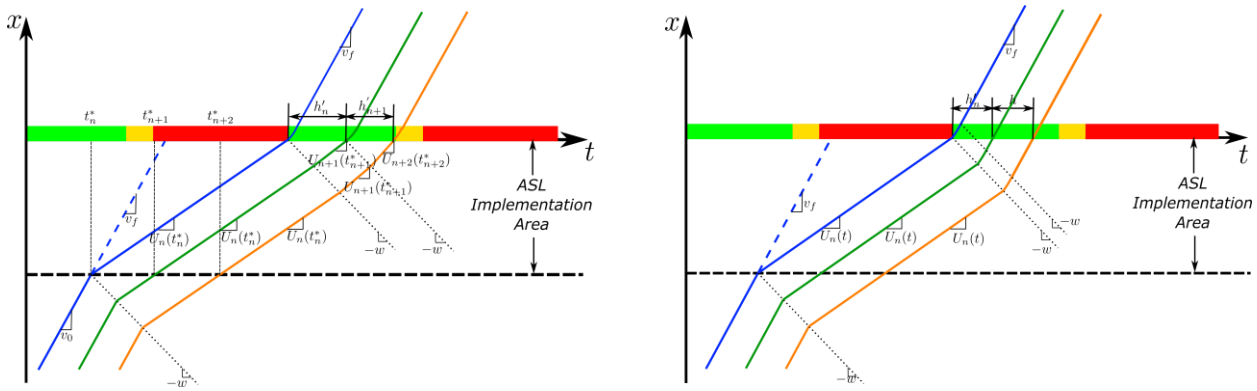

However, in the over-saturated condition, both implementations of the ASL may have little effect, as Figure 6c and Figure 6d show. The ASL for vehicle n is greater than the speed at which it enters the ASL implementation area, thus vehicle n will not be able to travel as expected. Instead, it will keep moving at its entering speed, denoted as v_0 in the figures (blue continuous lines). Correspondingly, vehicle $n+1$ and vehicle $n+2$ will also keep moving at v_0. Therefore, the headway between two adjacent vehicles can be reduced little.

Figure 6: Trajectories analysis of the ASL algorithm in the over-saturated condition

a) Trajectories of vehicles without control b) Fundamental diagram for calculating ASL

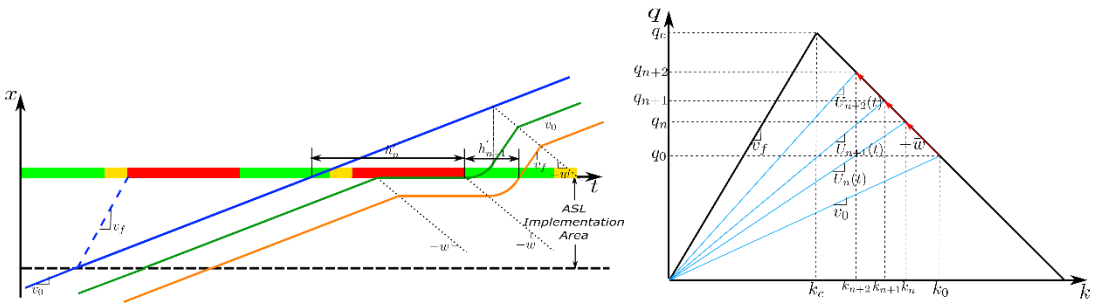

c) Trajectories after applying ASL statically d) Trajectories after applying ASL dynamically

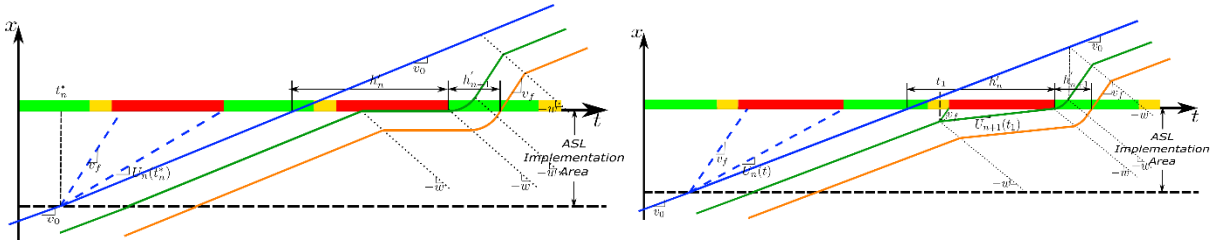

To summarize, from the two ASL implementations we can find that:

- Both the static ASL and the dynamic ASL can make vehicle trajectories smoother in both the under-saturated and saturated conditions.
- In both the under-saturated and saturated conditions, the dynamic ASL can reduce the accelerating process and the lost time at the intersection. However, the static ASL is unable to reduce the lost time.
- In the over-saturated condition, both the static ASL and the dynamic ASL are no more valid. Vehicles still need to experience a long accelerating process, and little lost time caused by start-up behaviors can be reduced.

4. Driving behavior models and evaluation indicators

In this chapter, we first introduce the car-following models that are used to simulate vehicle movements. We then discuss the start-up and clearance behaviors at signalized intersections. Furthermore, we introduce the indicators we adopt, i.e., network fundamental diagrams (NFDs) and fuel consumption, for evaluating the algorithm performance.

4.1 Driving behavior models

4.1.1 BA Newell's car-following model

We first introduce the BA Newell's car-following model (Jin & Laval, 2018) which was developed based on the Newell's car-following model (Newell, 1961) (Newell, 2002) by considering the real speed-up behaviors. Because BA Newell's car-following model is mathematically tractable and the speed limit is one parameter to decide the speed, thus ASL can be simply incorporated using it. The BA Newell's car-following model (Jin & Laval, 2018) can be written as follows:

$$v_n(t+\Delta t) = \min\left\{\frac{x_{n-1}(t) - x_n(t) - \zeta}{\tau}, v_f, v_n(t) + \Delta t a_0\right\}, \quad (7.)$$

where v_f is the original speed limit, $\tau = 1/(wk_j)$ is the time gap, k_j is the jam density, $\zeta = 1/k_j$ is the jam spacing, and a_0 is the bounded acceleration. In the BA Newell's car-following model, all the vehicles are assumed to move on a homogeneous road. The trajectory of the following vehicle is the same as that of the front vehicle, and all the vehicles will maintain minimum spaces and time gaps between themselves and the preceding vehicles.

4.1.2 Simplified Gipps model

The Gipps model (Gipps, 1981) is proposed based on the idea of pursuing a safe distance from the front vehicle to avoid collisions. Its speed can be calculated based on the idea that (1) vehicles do not exceed the desired speed; (2) vehicles seek to specify a safe following distance within which a collision would be unavoidable. (Treiber & Kesting, 2013) assumed the speed to be a constant within the reaction time, and presented the simplified Gipps model, which can be written as follows:

$$v_n(t+\Delta t) = \min\left\{v_f, v_n(t) + \Delta t a_0, -\Delta t b + \sqrt{\Delta t^2 b^2 + 2b[x_{n-1}(t) - x_n(t) - \zeta] + v_{n-1}(t)^2}\right\}, \quad (8.)$$

where Δt is the update time-step size, which is usually set as the reaction time, and b is the bounded deceleration.

4.1.3 Krauss model

The Krauss model (Krauss, et al., 1997) (Krauss, 1998) directly calculates the velocity as follows:

$$v_n(t+\Delta t) = \max\{0, v_{des,n}(t+\Delta t) - \varepsilon\}, \quad (9.)$$

where $v_{des,n}(t)$ is the desired velocity and ε is a random perturbation. $v_{des,n}$ is calculated according to the safe velocity, $v_{safe,n}$, as follows:

$$v_{des,n}(t+\Delta t) = \min\{v_f, v_n(t) + \Delta t a_0, v_{safe,n}(t+\Delta t)\}, \quad (10.)$$

$$v_{safe,n}(t+\Delta t) = v_{n-1}(t) + \frac{x_{n-1}(t) - x_n(t) - l_{n-1} - v_{n-1}(t)t_{re}}{\frac{v_{n-1}(t)+v_n(t)}{2b} + t_{re}}, \quad (11.)$$

where l_{n-1} is the length of vehicle $n-1$, t_{re} is the driver's reaction time and a_0 and b are still the desired acceleration and deceleration, respectively.

4.1.4 Decision process

- Start-up behaviors are influenced by bounded acceleration and reaction time. “Reaction time" is defined as the interval of time between the onset of the stimulus and the initiation of the response in the condition that someone has been told to react as rapidly as possible (Teichner, 1954). Because of reaction time, when the signal changes to green from red, the first stopping vehicle will maintain its current status for some time until it reacts to external changes.

- Before introducing clearance behaviors, the dilemma zone should be eliminated. The dilemma zone is widely known as an area on the high-speed intersection approach, where vehicles can neither safely stop before the stop line nor proceed through the intersection during the yellow interval (Gazis, et al., 1960). It can be eliminated as follows:

$$Y \geq t_{re} + \frac{v_f}{2b} + \frac{L_{int}}{v_f} \quad (12.)$$

where L_{int} is the length of the intersection, Y is the yellow plus all-red interval, t_{re} is the reaction time, and b is the bounded deceleration. We assume L is road length, x_{int} is the position of the intersection, $x_n(t)$ and $v_n(t)$ are the position and the speed of vehicle n at time t respectively. Then the conditions when a vehicle can go through the intersection and when it can stop can be written as follows (Morales Fresquet & Jin, 2018):

$$x_{int} - x_n(t) \geq t_{re} v_n(t) + \frac{v_n(t)^2}{2b}, \quad (13.)$$

$$x_{int} + L_{int} - x_n(t) < v_n(t) Y, \quad (14.)$$

There may be some vehicles that are able to both stop and cross, and we consider two types of drivers: aggressive drivers and non-aggressive drivers. Aggressive drivers will stop only if they cannot go through the intersection, nevertheless, non-aggressive drivers will stop once they satisfy the stop condition. It should also be noted that bounded deceleration b is only considered in the decision process of clearance behaviors. However, in the implementation process, deceleration is possible to be larger. We assume that the dilemma zone is eliminated. Every time when the signal changes to yellow from green, the decision process of drivers can be illustrated in Figure 7.

Figure 7: Decision process when the signal changes to yellow from green

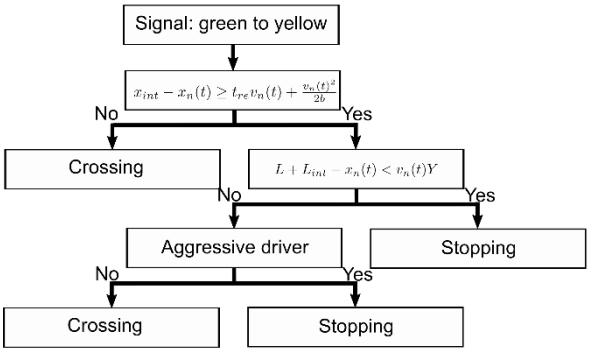

4.2 Network fundamental diagram (NFD) and emission model

4.2.1 The detection of speed periodicity

NFDs should be calculated after the system reaches stationary states. (Jin, et al., 2013) defined stationary states as asymptotic periodic traffic patterns. (Jin & Yu, 2015) found that periods should be the cycle length B or multiples of the cycle length in stationary states at signalized networks. Therefore, we can detect the period of the average speed in each cycle rather than the period of the original speed profile directly, which significantly reduces calculation costs. The average speed of vehicle n in the mth cycle can be calculated as follows:

$$\bar{v}_{ind,n}(m) = \frac{x_n\big((m+1)B\big) - x_n(mB)}{B}, \tag{15.}$$

where $x_n\big((m+1)B\big) - x_n(mB)$ means the distance vehicle n can cover in the mth cycle. The system average speed in the mth cycle is the sum of all the individual average speeds in such a cycle over the number of vehicles. It can be calculated as follows:

$$\bar{v}_{sys}(m) = \frac{\sum_{n=0}^{n=N} \bar{v}_{ind,n}(m)}{N}, \tag{16.}$$

where N is the total number of vehicles. We assume there are M cycles during the whole simulation duration and use m to represent the number which can be shifted along with the cycle numbers and m is shifted forward from the last cycle. We shift m along with up to 50 cycle numbers for calculating periods. If there exists some integers i that can satisfy the following equations for any m:

$$\max_{m = M-50, M-49, \ldots, M-1, M} \left| \bar{v}_{ind,n}(m) - \bar{v}_{ind,n}(m-i) \right| < \epsilon \quad (17.)$$

$$\max_{m = M-50, M-49, \ldots, M-1, M} \left| \bar{v}_{sys}(m) - \bar{v}_{sys}(m-i) \right| < \epsilon \quad (18.)$$

where ϵ is a small enough number. we consider that those integers are the periods of individual speed or system average speed for corresponding cycle length B and number of vehicles N. The final i is the smallest number among these integers.

We consider that N vehicles keep moving on a closed ring road, and the period of vehicle n's speed is denoted as $T_n(N)$. We find that periods of different individuals are the same under one specific density, and this can be clarified with an example. We assume the $N = 20$, free-flow speed is $12m/s$, and the cycle length is $60s$ ($24s$ green, $6s$ yellow, and $30s$ red). We plot the speed profiles of vehicle 1 and vehicle 20, as Figure 8a shows. The periods for speeds of both vehicles are $20B$. In addition, after shifting back the speed profile of vehicle 1, it coincides with that of vehicle 20, as Figure 8b shows. Therefore, we can consider that all the vehicles cover the same distance and experience the same moving pattern in $T_n(N)$. However, such periods may not be the same as the period of the system average speed $T_{sys}(N)$. With the above settings, the period of the system average speed is B. With more experiments, we find that periods of the system average speed are much smaller and more stable than periods of individual speeds. Therefore, when calculating network fundamental diagrams, we calculate the average flow rate at corresponding densities with the system average speed.

Figure 8: Speed profiles in the last two individual periods

a) Speed profiles of vehicle 1 and vehicle 20

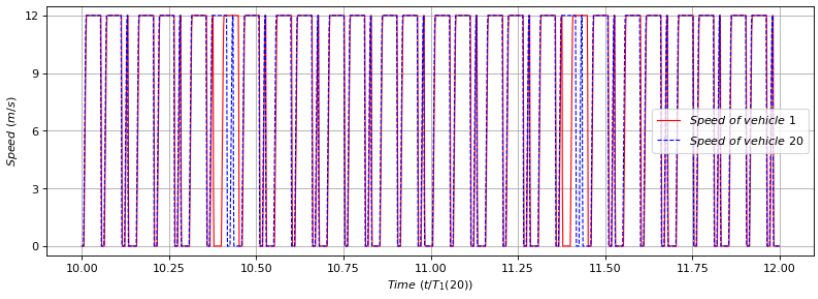

b) Speed profiles of shifted vehicle 1 and vehicle 20

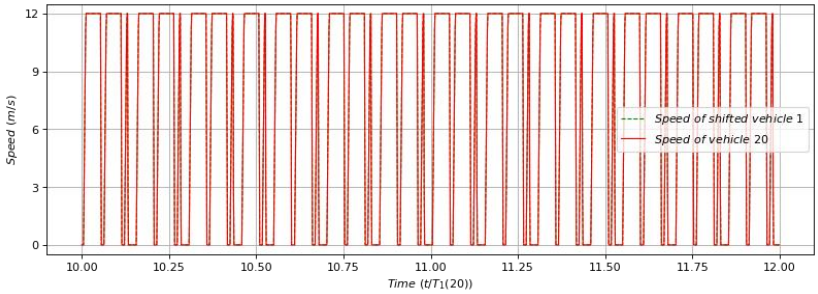

4.2.2 Network fundamental diagram

The network fundamental diagram (NFD) of a system is a diagram that gives a relation between the average traffic flow and average traffic density (Godfrey, 1969). It is chosen to evaluate the impact on system mobility of our algorithm. In this simulation, the simulation duration σ of all the vehicles are the same. We assume there are N vehicles in the system. The density can be calculated through:

$$\bar{k}(N) = \frac{N}{L}, \tag{19.}$$

and the system average speed in $T_{sys}(N)$ can be calculated as follows:

$$\bar{v}(N) = \frac{\sum_{m=M-T_{sys}(N)}^{m=M} \bar{v}_{sys}(m)}{T_{sys}(N)}, \tag{20.}$$

where $T_{sys}(N)$ is the period of the system average speed (the unit is the cycle) and M is the number of cycles during the simulation duration. Thus, the flow rate can be calculated through:

$$\bar{q}(N) = \bar{k}(N)\bar{v}(N). \tag{21.}$$

(Jin, Wen-Long, 2015) derived theoretical results for the NFD on a signalized road. Instead of a triangular fundamental diagram, the fundamental diagram will be approximated by a piecewise linear function. Compared with a single point of the maximum flow rate when there is no signal, on a signalized road, the maximum flow rate will be a horizontal line segment, as Figure 9 shows, where π is the phase ratio and q_c is the saturation flow rate when there is no signal.

Figure 9: The representation of the network fundamental diagram

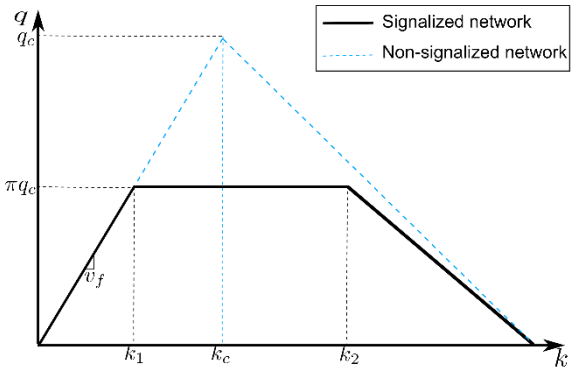

4.2.3 VT-micro model for estimating fuel consumption

In consideration of simplicity, accuracy, and ease of implementation, we use the Virginia Tech Microscopic Energy and Emission Model (VT-Micro model) to describe environmental influence (Ahn, et al., 2002). It is a regression model which considers a combination of linear, quadratic, and cubic speed and acceleration terms. We utilize fuel consumption to indicate the environmental impacts of our algorithm. Lower fuel consumption corresponds to environmental improvement. This model provides the least number of terms with a relatively good fit to the original data (R^2 in excess of 0.92 for all measures of effectiveness (MOE)). The model has the following form:

$$MOE_e(t,n) = \begin{cases} e^{\sum_{i=0}^{i=3}\sum_{i=3}^{i=3} L_{i,j}^{e} v_n(t)^i a_n(t)^i}, & \text{if } a_n(t) \geq 0 \\ e^{\sum_{i=0}^{i=3}\sum_{i=3}^{i=3} F_{i,j}^{e} v_n(t)^i a_n(t)^i}, & \text{if } a_n(t) < 0 \end{cases} \quad (22.)$$

where $MOE_e(t,n)$ is instantaneous fuel consumption (l/s) of vehicle n at time t, $L_{i,j}^{e}$ and $F_{i,j}^{e}$ are regression model coefficients for MOE `$e$' at speed power `i' and acceleration power `j', $v(t,n)$ is instantaneous vehicle speed (km/h), and $a(t,n)$ is instantaneous vehicle acceleration $(km/h/s)$. To create a simple enough condition, the vehicles utilized in our system are assumed to be composite, and the coefficients we utilize are the averages of 9 vehicle categories, as Table 2 and Table 3 show.

Table 2: Positive Acceleration Coefficient

Coefficient	Constant	Acceleration	Acceleration^2	Acceleration^3
Constant	7.734520000	0.229460000	-0.005610000	0.000097730
Speed	0.027990000	0.006800000	-0.000772210	0.000008380
Speed^2	-0.000222800	-0.000044020	7.90000×10^{-7}	8.17000×10^{-7}
Speed^3	1.09000×10^{-6}	4.80000×10^{-8}	3.27000×10^{-8}	-7.79000×10^{-9}

Table 3: Negative Acceleration Coefficient

Coefficient	Constant	Acceleration	Acceleration^2	Acceleration^3
Constant	-7.734520000	-0.017990000	-0.004270000	0.000188290
Speed	0.028040000	0.007720000	0.000837440	0.000033870
Speed^2	-0.000219880	-0.000052190	-7.44000×10^{-7}	2.77000×10^{-7}
Speed^3	1.08000×10^{-6}	2.47000×10^{-8}	4.87000×10^{-8}	3.79000×10^{-9}

As mentioned above, all the vehicles have the same individual periods and cover the same distance during one individual period in stationary states. Therefore, we use the average fuel consumption of vehicle 1 to move one unit distance in one individual period to represent the fuel consumption level. Considering the computation cost, we choose 50 cycles, which is long enough and only results in a small and acceptable error, as the upper boundary of individual periods. It means that if periods are larger than 50 cycles, we calculate the average fuel consumption during 50 cycles. The total fuel consumption of the first vehicle in one period is the sum of the instantaneous fuel consumption, as follows:

$$V_1 = \sum_{t_{step}=\frac{\sigma-z}{\Delta t}}^{t_{step}=\frac{\sigma}{\Delta t}} MOE_e\left(t_{step}\Delta t, 1\right)\Delta t\,. \tag{23.}$$

The corresponding distance the vehicle has covered can be calculated through:

$$d_1 = x_1(\sigma) - x_1(\sigma - z), \tag{24.}$$

$$z = \begin{cases} T_1(N)B, & if\ T_1(N) \le 50 \\ 50B, & if\ T_1(N) > 50 \end{cases}$$

where σ is the simulation duration, $T_1(N)$ is the individual period of vehicle 1 (its unit is the cycle length), N is the total number of vehicles in the system (it can represent congestion levels), Δt is the time-step size, t_{step} is time in the unit of time step-size. To move a certain distance d_1, the fuel we need is V_1. Thus, the quotient of the two represents the fuel required for a car to travel per unit distance, as follows:

$$\bar{V}_1 = \frac{V_1}{d_1}. \tag{25.}$$

5. Numerical example

5.1 Simulation setup

To begin with, we build the simulation system, and the parameters settings are listed in Table 4.

Table 4: Settings of the simulation

Parameters	Values	Parameters	Values
Road length L	$720m$	ASL implementation area D	$300m$
Minimum clearance s_0	$2m$	Vehicle length l_n	$5m$
Jam spacing ζ	$7m$	Time gap τ	$1.5s$
Reaction time t_{re}	$0.5s$	Cycle length B	$60s$
Green interval G	$24s$	Yellow plus all-red interval Y	$6s$
Red interval R	$30s$	Phase ratio π	0.5
Free-flow speed v_f	$12m/s$	Bounded acceleration a_0	$1.5m/s^2$
Bounded deceleration b	$3m/s^2$	Acceptable error range ϵ	10^{-5}

We construct a signalized ring road with one lane and one typical three-color traffic light. It is equivalent to a fixed segment, on which there is inexhaustible traffic flow. We assume all drivers are aggressive. Initially, vehicles are evenly distributed on the ring road and labeled in a counterclockwise direction. After the simulation begins, the signal starts with a green interval, and vehicles move clockwise. When the signal turns from red to green, the first stopping vehicle's reaction time is $1.5sec$. We set Δn to be 1 and traverse the density from 0 to near k_j. Based on the system we have created the jam density $k_j = \frac{1}{\zeta} = \frac{1}{7}\ veh/m$, thus the simulation starts from 2 vehicles to 101 vehicles.

5.2 Results of system mobility

Network fundamental diagrams of three car-following models are shown in Figure 10. It can be found that the impact of our algorithm shows similar patterns for all three models. The static ASL makes no difference in the under-saturated condition, but it reduces system mobility in the saturated condition compared to the cases without control. Applying the dynamic ASL can increase system mobility in the saturated condition. However, it cannot contribute to system mobility in the under-saturated or the over-saturated conditions. These are consistent with our anticipation in Section 3.2 that lost time may increase.

Figure 10: NFDs of different car-following models

a) BA Newell's model b) Simplified Gipps model c) Krauss model

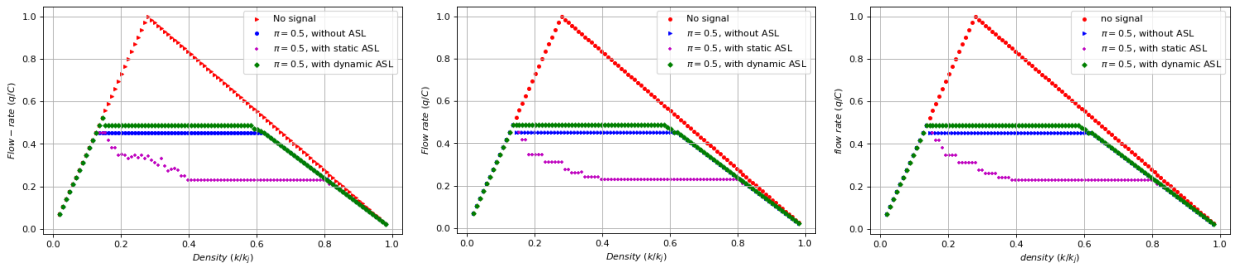

We plot vehicle trajectories of three models in the last five cycles when 1. there is no ASL; 2. the static ASL is applied; 3. the dynamic ASL is applied. Because ASL mainly function in the saturated condition, we choose 50 vehicles, which corresponds to about $0.5k_j$, as an example. The signals are plotted at the beginning and the end of the road, and note that the green represents the phase, including green and yellow plus red intervals. The trajectories are shown in Figure 11. The magenta and blue trajectories clearly show that when there is no control or when the static ASL is applied, vehicles must still stop before the intersection, and the lost time cannot be reduced. From the cyan trajectories, we can see that vehicles directly accelerate from the ASL, shortening the acceleration process and resulting in reduced start-up time and smoother trajectories.

Figure 11: Vehicle trajectories in the last 5 cycles

a) BA Newell's car-following model

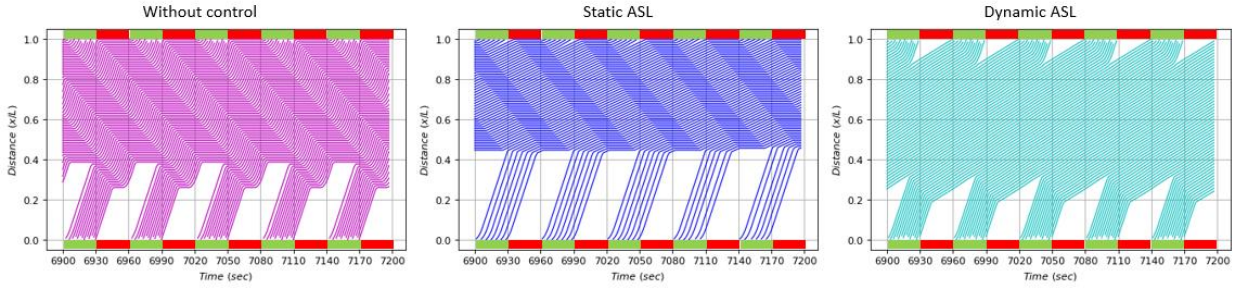

b) Simplified Gipps model

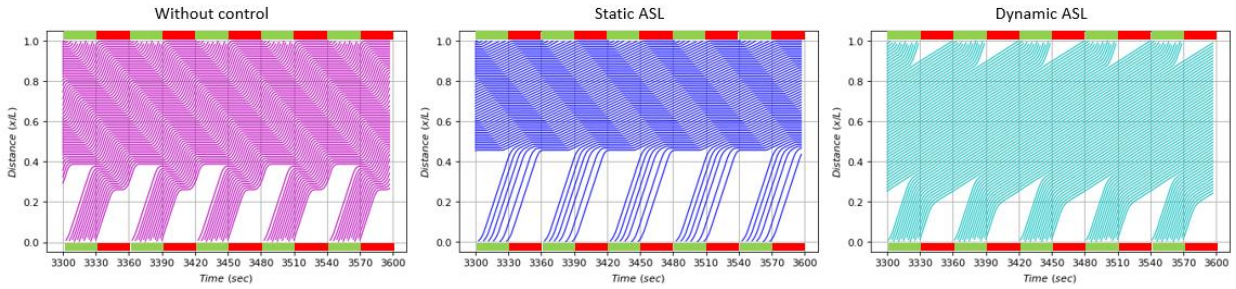

c) Krauss model

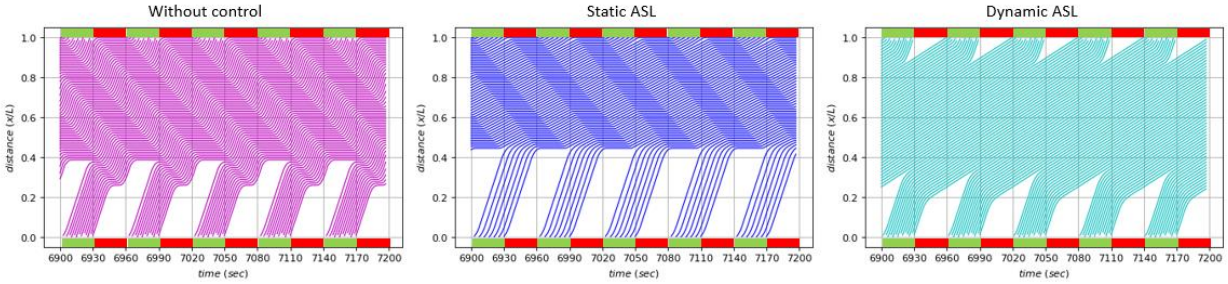

5.3 Results of fuel consumption

We choose fuel consumption to measure environmental impacts and utilize the VT-micro model to calculate it. We assume all the vehicles are connected and discuss the conditions of all these models. Considering the reality, we set the upper boundary of fuel consumption for a vehicle (either a connected vehicle or a non-connected vehicle) to cover a unit distance to be 50 liters. Because 50 liters is the capacity of many fuel tanks, and $50l/m$ means that the vehicle uses up all the fuel immediately. Therefore, when the calculated fuel consumption is larger than $50l/m$, we consider it to be $50l/m$. Because network fundamental diagrams have shown that the static ASL can have a negative effect on system mobility, we no longer discuss the static ASL here.

The reduction rates of fuel consumption versus relative densities are plotted in Figure 12. We fitted the trend of fuel consumption versus densities through nonlinear regression. The performance of our algorithm in the three models is still similar. In addition, the impact of the dynamic ASL has similar trends from the perspectives of system mobility and fuel consumption. It has the best performance in the saturated condition, and the reduction rate (the proportion of the fuel that can be saved through the dynamic ASL) can reach up to about 45%.

Figure 12: Reduction of fuel consumption of different car-following models

a) BA Newell's model

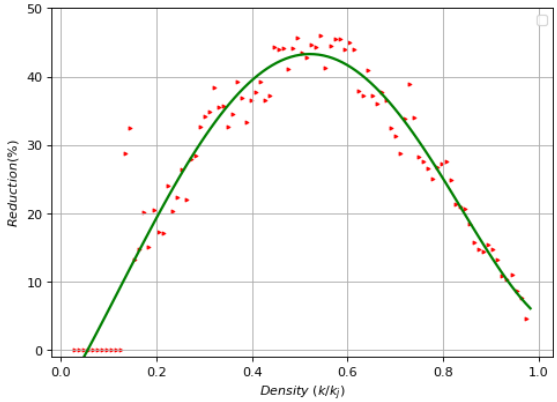

b) Simplified Gipps model

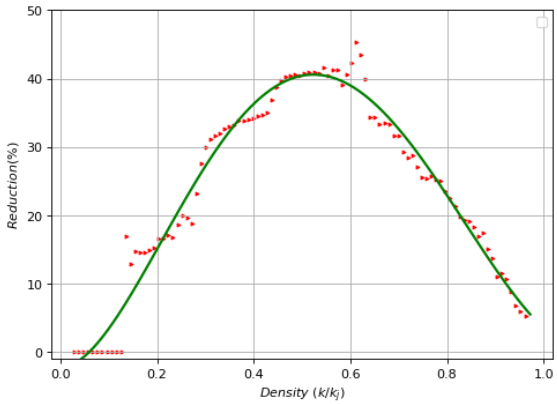

c) Krauss model

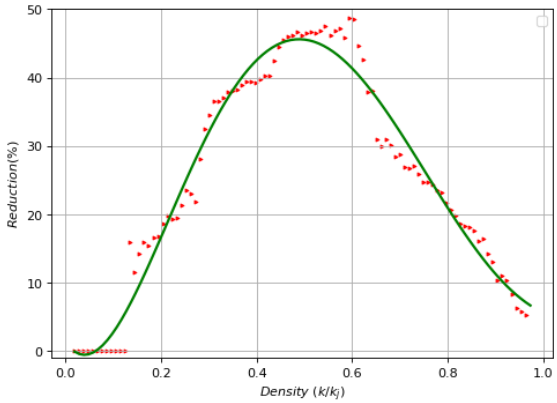

6. Impacts of market penetration rates (MPRs) and ASL implementation areas

In this chapter, we detect the effect of our algorithm under different MPRs and ASL implementation areas. We adopt the Krauss model to apply our algorithm and show how the algorithm can increase system mobility and reduce fuel consumption with different MPRs and ASL implementation areas.

6.1 Impact of MPRs

In our study, we consider the MPR as the probability of a vehicle in the system being a connected vehicle. For one density and one MPR, the number of connected vehicles in the system is fixed, but the distribution of connected vehicles and non-connected vehicles is random. That is, some random elements are added to the system, and simulation results may be different from time to time. Therefore, we use Monte Carlo simulation (Mooney, 1997) (Raychaudhuri, 2008). We simulate ten times at each density point and calculate the average.

We take 0.1, 0.5, 0.7, and 1 MPRs of connected vehicles as examples. The results are shown in Figure 13. From the perspectives of both system mobility and fuel consumption, in the cases of different MPRs, the ASL algorithm mainly plays a role in the saturated condition. Neither under-saturated condition nor over-saturated condition can it fully function. From Figure 13a we can see that the improvement rate of system mobility is not obvious when the MPR is low. When the MPR is 0.1, the corresponding NFD shows little difference. However, when the MPR increases to 0.5 or 0.7, we can see more improvement in system mobility through corresponding NFDs. When the MPR is 1, system mobility can be further improved. Impacts to fuel consumption under different MPRs are shown in Figure 13b. We can see a substantial reduction in fuel consumption when the MPR is only 0.1, and a higher MPR leads to more reduction. 0.5 MPR can lead to as much as 40% fuel consumption reduction and when the MPR increases to 1, about 45% of fuel can be saved.

To conclude, the results about MPRs conform to the rules of our algorithm: it should work even when there is only one connected vehicle in the system, but with a higher MPR, it should have better performance.

Figure 13: NFDs and fuel consumption reduction of the dynamic ASL under different MPRs

a) Network fundamental diagram

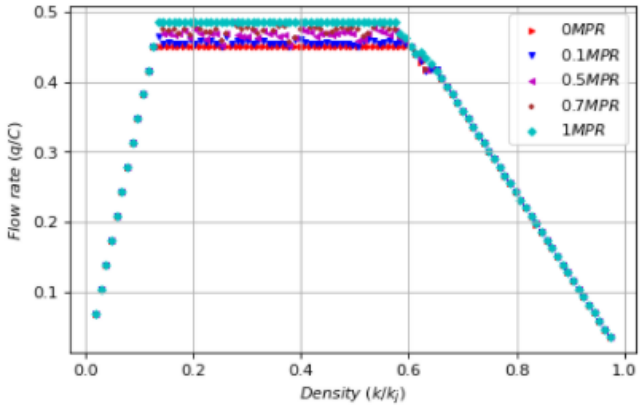

b) Fuel consumption reduction

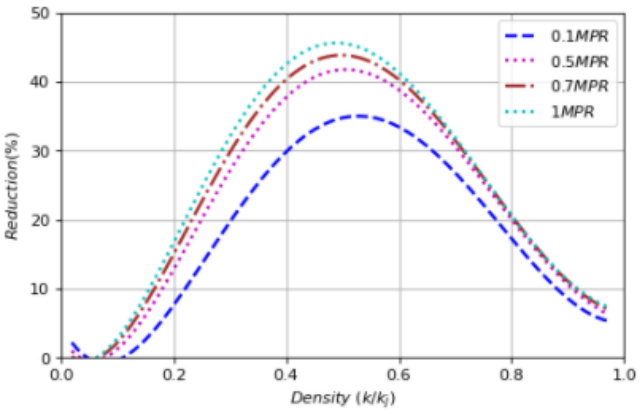

Vehicle trajectories under different MPRs are plotted in Figure 14. We still take vehicle number is 50 as an example. It should be noted that as mentioned above, some stochastic elements exist in our simulation when considering MPRs, thus vehicle trajectories are only a sample. We plot vehicle trajectories in the last five cycles when MPRs are 0.1, 0.5, 0.7, and 1. From trajectories we can see that the trajectories are smoother and stopping time can already be reduced to a great extent when the MPR is only 0.1, and with the increase of MPRs, stopping time can be further reduced. In the cases when MPRs are low, stopping behaviors cannot be eliminated and many vehicles still need to accelerate from zero when going through the intersection, and the accelerating process cannot be shortened. Thus, from the perspective of system mobility, the effect of ASL is relatively limited when MPRs are very low.

To summarize, ASL can make trajectories smoother, and the degree to which trajectories become smoother is positively related to MPRs. Therefore, the improvement rate of system mobility and the reduction of fuel consumption is also positively related to MPRs.

Figure 14: Vehicle trajectories in the last 5 cycles under different MPRs

a) MPR=0.1

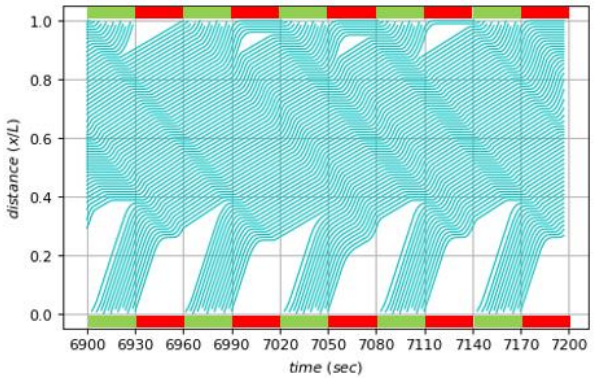

b) MPR=0.5

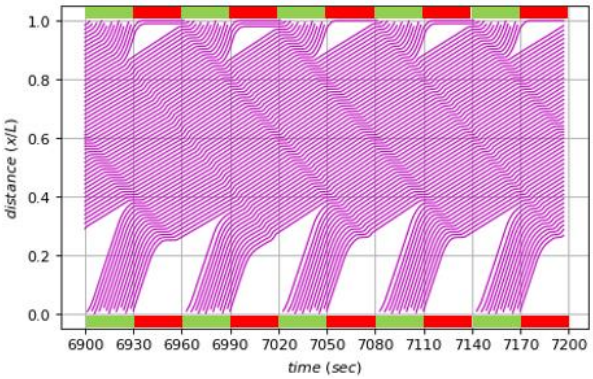

a) MPR=0.7

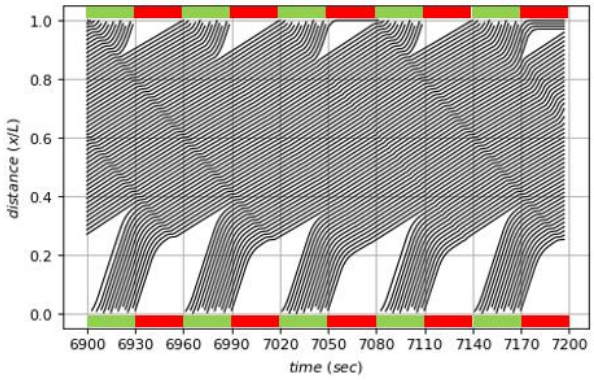

b) MPR=1

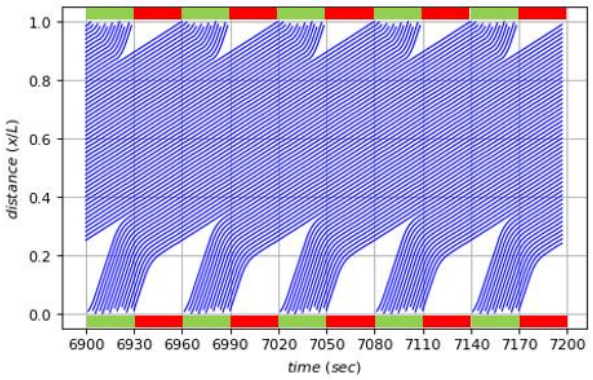

6.2 Impact of ASL implementation areas

Our study has proved that our ASL algorithm can contribute to the system when the ASL implementation area is 300 meters. The control group, that is, the case where no algorithm is applied can be regarded as the condition where the ASL implementation area is zero.

Although increasing the ASL implementation area may improve the algorithm's performance, a larger ASL implementation area will result in higher communication and computation costs. Therefore, our principle for selecting the ASL implementation area is to reduce the computation and communication cost as much as possible while guaranteeing the efficacy of ASL algorithms. The selection of the ASL implementation area can be formulated as an optimization problem as follows:

$$\min D \quad s.t. \begin{cases} D \leq 300, \\ D \geq 0, \\ |\bar{V}_1(D) - \bar{V}_1(300)| \leq \epsilon, \\ |q_c(D) - q_c(300)| \leq \epsilon, \end{cases} \tag{26.}$$

where D is the length of the ASL implementation area, thus it should be in the range of 0 to the maximum transmission range $300m$. $\bar{V}_1(D)$ is the average fuel consumption for vehicle 1 to move a unit distance in one period when the ASL implementation area is D, and $q_c(D)$ is the capacity of the system when the ASL implementation area is D. Therefore, the third and the fourth constraints mean that when the length of the ASL implementation area is D, the improvement in system mobility and the reduction in fuel consumption is almost the same as when it is $300m$.

We assume the MPR is 1 and solve this problem through simulation. Because we have found that this algorithm mainly works in the saturated condition, we take vehicle numbers equal to 20, 30, 40, and 50 as examples. We change the ASL implementation area from $10m$ to $300m$ at intervals of $10m$.

The results are shown in Figure 15. From the results, we can see that the system mobility improvement and fuel consumption reduction show the same tendency along the ASL implementation area. When the ASL implementation area is larger than certain values, system mobility improvement and fuel consumption reduction are stable, and the algorithm can fully function. For system mobility, it can no longer be improved when the ASL implementation area is shorter than $50m$. The reduction in fuel consumption gradually disappears when such an area is smaller than $100m$. Considering all the conditions, to guarantee control results as well as reduce computation cost, we recommend the ASL implementation area to be approximate $100m$.

Figure 15: System mobility improvement and fuel consumption reduction with different ASL implementation areas

a) System mobility

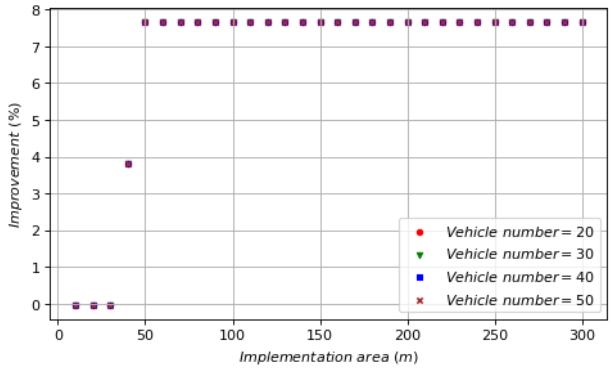

b) Fuel consumption

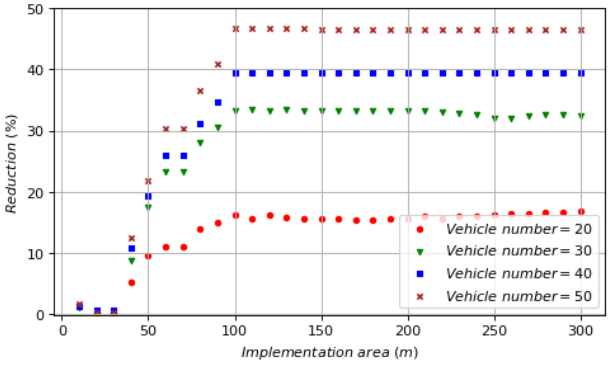

7. Conclusion

In this project, we formulate and analyze a heuristic hierarchical ASL algorithm based on the idea in (Ubiergo & Jin, 2016) that all the vehicles enter the intersection at saturation headway intervals. The entire algorithm consists of three steps: 1. we calculate the desired arrival time based on the original speed limit; 2. we calculate the desired arrival time based on the minimum headway to front vehicles; 3. we calculate the ASL with the desired arrival time and the distance to the intersection. We consider two implementations of the algorithm: the static ASL and the dynamic ASL.

We first theoretically analyze the effects of our algorithm on vehicle trajectories with the two implementations at different congestion levels and find that the lost time not only will not decrease but may increase with the static ASL, while the dynamic ASL can reduce the lost time and eliminate stopping behaviors. We then apply our algorithm with the BA Newell's car-following model, the Gipps model, and the Krauss model, and propose the use of network fundamental diagrams and fuel consumption to evaluate the efficacy of our algorithm. The fundamental diagrams show that the static ASL has negative effects on system mobility, while the dynamic ASL can improve system mobility. Especially in the saturated condition, system mobility increases by nearly 10%. These findings are consistent with our analysis. The fuel consumption of one vehicle to move a unit distance also decreases after applying the dynamic ASL. Our algorithm still has the best performance in the saturated condition, where the fuel consumption can be reduced by up to 45%.

In addition, we study how MPRs and ASL implementation areas can influence the efficacy of our algorithm. In general, the efficacy of our algorithm improves with the increase of MPRs, however, even with 0.1 MPR, our algorithm can substantially reduce fuel consumption. We also proposed a recommendation for the ASL implementation area to be about 100 meters, which can not only guarantee algorithm efficiency but also reduce communication and computation costs.

But our study still has certain limitations. We consider that not only MPRs can influence the efficiency of our algorithm. Firstly, we only consider the one-lane scenario and assume that vehicles are first-in-first-out (FIFO). However, when we consider the multilane scenario where lane-changing and overlapping may happen, the performance of our algorithm may be different, and evaluating the performance of our algorithm in the multilane scenario is one extension of this study. Under one MPR, the distribution of connected vehicles and non-connected vehicles may also impact how our algorithm can function, and this can also be one extension of this study. Besides, we can consider different categories of vehicles, things like buses and trucks, and explore what effect our algorithm will have on different categories of vehicles. In addition, the numerical analysis of our algorithm in this study is based on

simulations with car-following models, while we consider applying our algorithm to real vehicles or to scaled-down vehicle models in the future to provide a more comprehensive evaluation of our algorithm.

References

Agency, U. S. E. P., 2018. *Sources of Greenhouse Gas Emissions.* [Online]
Available at: https://www.epa.gov/ghgemissions/sources-greenhouse-gas-emissions\#transportation
[Accessed 2018].

Ahn, K. & Rakha, H., 151-167. The effects of route choice decisions on vehicle energy consumption and emissions. *Transportation Research Part D,* Volume 13, p. 2008.

Ahn, K., Rakha, H., Trani, A. & Van Aerde, M., 2002. Estimating vehicle fuel consumption and emissions based on instantaneous speed and acceleration levels. *Journal of transportation engineering,* Volume 128, pp. 182-190.

Alam, M. S. a. M. A., 2014. A critical review and assessment of Eco-Driving policy & technology: Benefits & limitations. *Transport Policy,* Volume 35, pp. 42-49.

Anandarajah, G., McDowall, W. & Ekins, P., 2013. Decarbonising road transport with hydrogen and electricity: Long term global technology learning scenarios. *International Journal of Hydrogen Energy,* Volume 38, pp. 3419-3432.

Barkenbus, J. N., 2010. Eco-driving: An overlooked climate change initiative. *Energy policy,* Volume 38, pp. 762-769.

Barth, M. et al., 2000. The development of a comprehensive modal emissions model. *NCHRP Web-only document,* Volume 122, pp. 25-11.

Cheah, . L. W. et al., 2009. The trade-off between automobile acceleration performance, weight, and fuel consumption. *SAE International Journal of Fuels and Lubricants,* Volume 1, pp. 771-777.

Chen, R., Zhang, T. & Levin, M. W., 2020. Effects of Variable Speed Limit on Energy Consumption with Autonomous Vehicles on Urban Roads Using Modified Cell-Transmission Model. *Journal of Transportation Engineering, Part A,* Volume 146, p. 04020049.

Coppola, R. & Morisio, M., 49. Connected car: technologies, issues, future trends. *ACM Computing Surveys (CSUR),* Volume 49, pp. 1-36.

Eckhoff, D., Halmos, B. & German, R., 2013. *Potentials and limitations of green light optimal speed advisory systems.* s.l., s.n.

Gazis, D., Herman, R. & Maradudin, A., 1960. The problem of the amber signal light in traffic flow. *Operations research,* Volume 8, pp. 112-132.

Gipps, P. G., 1981. A behavioural car-following model for computer simulation. *Transportation Research Part B,* Volume 15, pp. 105-111.

Godfrey, J., 1969. The mechanism of a road network. *Traffic Engineering & Control,* Volume 8.

Huang, Y., Hong, G. & Huang, R., 2015. Investigation to charge cooling effect and combustion characteristics of ethanol direct injection in a gasoline port injection engine. *Applied energy,* Volume 160, pp. 244-254.

Jin, Wen-Long, Y. Y., 2015. Performance analysis and signal design for a stationary signalized ring road. *arXiv preprint arXiv:1510.01216.*

Jin, W.-L., Gan, Q.-J. & Gayah, V. V., 2013. A kinematic wave approach to traffic statics and dynamics in a double-ring network. *Transportation Research Part B,* Volume 57, pp. 114-131.

Jin, W.-L. & Laval, J., 2018. Bounded acceleration traffic flow models: A unified approach. *Transportation Research Part B,* Volume 111, pp. 1-18.

Jin, W.-L. & Yu, Y., 2015. Performance analysis and signal design for a stationary signalized ring road. *arXiv preprint arXiv:1510.01216.*

Katsaros, K., Kernchen, R., Dianati, M. & Rieck, D., 2011. *Performance study of a Green Light Optimized Speed Advisory (GLOSA) application using an integrated cooperative ITS simulation platform.* s.l., s.n.

Kenney, J. B., 2011. Dedicated short-range communications (DSRC) standards in the United States. *Proceedings of the IEEE,* Volume 99, pp. 1162-1182.

Keyvan-Ekbatani, M., Kouvelas, A., Papamichail, I. & Papageorgiou, M., 2012. Exploiting the fundamental diagram of urban networks for feedback-based gating. *Transportation Research Part B,* Volume 46, pp. 1393-1403.

Khondaker, B. & Kattan, L., 2015. Variable speed limit: A microscopic analysis in a connected vehicle environment. *Transportation Research Part C,* Volume 58, pp. 146-159.

Krauss, S., 1998. Microscopic modeling of traffic flow: Investigation of collision free vehicle dynamics.

Krauss, S., Wagner, P. & Gawron, C., 1997. Metastable states in a microscopic model of traffic flow. *Physical Review E,* Volume 55, p. 5597.

Mandava, S., Boriboonsomsin, K. & Barth, M., 2009. *Arterial velocity planning based on traffic signal information under light traffic conditions.* s.l., s.n.

McShane, W. R. & Roess, R. P., 1990. *Traffic engineering.* s.l.:s.n.

Milikowsky, B., 2013. *Building America's Future: Falling Apart and Falling Behind.* s.l.:Building America's Future Educational Fund.

Mooney, C. Z., 1997. *Monte carlo simulation.* s.l.:Sage Publications.

Morales Fresquet, A. & Jin, W.-L., 2018. *Evaluating the impacts of start-up and clearance behaviors in a signalized network: A network fundamental diagram approach,* s.l.: Universitat Polit'ecnica de Catalunya.

Newell, G. F., 1961. Nonlinear effects in the dynamics of car following. *Operations research,* Volume 9, pp. 209-229.

Newell, G. F., 2002. A simplified car-following theory: a lower order model. *Transportation Research Part B,* Volume 36, pp. 195-205.

others, N. R. C. a., 2000. *Modeling mobile-source emissions.* s.l.:National Academies Press.

Rakha, H. & Kamalanathsharma, R. K., 2011. *Eco-driving at signalized intersections using V2I communication.* s.l., s.n.

Raychaudhuri, S., 2008. *Introduction to monte carlo simulation.* s.l., s.n.

Seredynski, M., Mazurczyk, W. & Khadraoui, D., 2013. *Multi-segment green light optimal speed advisory.* s.l., s.n.

Sivak, M. & Schoettle, B., 2012. Eco-driving: Strategic, tactical, and operational decisions of the driver that influence vehicle fuel economy. *Transport Policy,* Volume 22, pp. 96-99.

Teichner, W. H., 1954. Recent studies of simple reaction time. *Psychological Bulletin,* Volume 51, p. 128.

Treiber, M. & Kesting, A., 2013. Traffic flow dynamics. *Traffic Flow Dynamics: Data, Models and Simulation, Springer-Verlag Berlin Heidelberg.*

Ubiergo, G. A. & Jin, W.-L., 2016. Mobility and environment improvement of signalized networks through Vehicle-to-Infrastructure (V2I) communications. *Transportation Research Part C,* Volume 68, pp. 70-82.

Yang, H. & Jin, W.-L., 2014. A control theoretic formulation of green driving strategies based on inter-vehicle communications. *Transportation Research Part C,* Volume 41, pp. 48-60.

Zheng, N., Waraich, R. A., Axhausen, K. W. & Geroliminis, N., 2012. A dynamic cordon pricing scheme combining the macroscopic fundamental diagram and an agent-based traffic model. *Transportation Research Part A,* Volume 46, pp. 1291-1303.

Zhen, X. & Wang, Y., 2015. An overview of methanol as an internal combustion engine fuel. *Renewable and Sustainable Energy Reviews,* Volume 52, pp. 477-493.

Data Management Plan (Heading 1 style)

Products of Research

As a simulation-based study, the products of this project include:

1. A peer-reviewed research report.
2. A script for simulating the application of our algorithm

Data Format and Content

The research report will appear in a common document-viewing format, such as PDF, the script is written in Python, and a Jupyter notebook file will be provided.

Data Access and Sharing

The numerical study is based on simulation, and no personal data is used in the project, so there is no threat of identity theft. The jupyter notebook file can be accessed and downloaded from: https://github.com/ximeng96/Advisory-speed-limit-ASL-algorithm

Reuse and Redistribution

The research products' intellectual property rights are owned by the project's researchers, who also manage the data before their transfer to a data archive. Public agencies such as Caltrans have free and complete access to the research products. The team permits the use of research products with appropriate citation and credit to the research team and project.